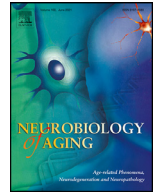


Contents lists available at ScienceDirect

Neurobiology of Aging

journal homepage: www.elsevier.com/locate/neuaging.org

Regular article

White matter hyperintensities are associated with grey matter atrophy and cognitive decline in Alzheimer's disease and frontotemporal dementia

Mahsa Dadar^{a,b,*}, Ana Laura Manera^{a,b}, Simon Ducharme^{b,c}, D. Louis Collins^{a,b}^a Neuroimaging and Surgical Tools Laboratory, Montreal Neurological Institute, McGill University, Montreal, QC, Canada^b McConnell Brain Imaging Centre, Montreal Neurological Institute, McGill University, Montreal, QC, Canada^c Department of Psychiatry, Douglas Mental Health University Institute and Douglas Research Centre, McGill University, Montreal, QC, Canada

ARTICLE INFO

Article history:

Received 12 July 2021

Revised 21 October 2021

Accepted 26 November 2021

Available online 3 December 2021

Keywords:

White matter hyperintensities

small-vessel disease

neurodegenerative disease

Alzheimer's disease

fronto-temporal dementia

Parkinson's disease

mild cognitive impairment

ABSTRACT

White matter hyperintensities (WMHs) are commonly assumed to represent non-specific cerebrovascular disease comorbid to neurodegenerative processes, rather than playing a synergistic role. We compared the impact of WMHs on grey matter (GM) atrophy and cognition in normal aging ($n = 571$), mild cognitive impairment (MCI, $n = 551$), Alzheimer's dementia (AD, $n = 212$), fronto-temporal dementia (FTD, $n = 125$), and Parkinson's disease (PD, $n = 271$). Longitudinal data were obtained from ADNI, FTLNDI, and PPMI datasets. Mixed-effects models were used to compare WMHs and GM atrophy between patients and controls and assess the impact of WMHs on GM atrophy and cognition. MCI, AD, and FTD patients had significantly higher WMH loads than controls. WMHs were related to GM atrophy in insular and parieto-occipital regions in MCI/AD, and frontal regions and basal ganglia in FTD. In addition, WMHs contributed to more severe cognitive deficits in AD and FTD compared to controls, whereas their impact in MCI and PD was not significantly different from controls. These results suggest potential synergistic effects between WMHs and proteinopathies in the neurodegenerative process in MCI, AD and FTD.

© 2021 Elsevier Inc. All rights reserved.

Alzheimer's Disease Neuroimaging Initiative¹
 Frontotemporal Lobar Degeneration Neuroimaging Initiative²

1. Introduction

White matter hyperintensities (WMHs), defined as nonspecific hyperintense regions in the white matter (WM) tissue of the brain on T2-weighted or Fluid-Attenuated Inversion Recovery (FLAIR) magnetic resonance images (MRIs) are common findings in the aging population (Hachinski et al., 1987). These age-related WMHs are considered to be the most common MRI signs of cerebral small-vessel disease and are generally due to chronic hypoperfusion and alterations in the blood brain barrier (McAleese et al., 2016) secondary to common vascular risk factors (e.g., hypertension, cigarette smoking, diabetes). However, there are several other pathological causes of WMHs including demyelination, axonal and neuronal loss, higher levels of microglial activation, inflammation, degeneration, and amyloid angiopathy (Abraham et al., 2016; Gouw et al., 2011).

In clinical dementia practice, these frequent WMHs are generally assumed to be a non-specific comorbid vascular contribution to cognitive decline. However, various evidence suggests that WMHs could play a more direct role in the progression

* Corresponding author at: Neuroimaging and Surgical Tools Laboratory, Montreal Neurological Institute, McGill University, 3801 University Street, Room WB320, Montréal, QC H3A 2B4. Tel.: 514-398-1573; fax: 514-398-8106.

E-mail address: mahsa.dadar@mcgill.ca (M. Dadar).

¹ Data used in preparation of this article were obtained from the Alzheimer's Disease Neuroimaging Initiative (ADNI) database (adni.loni.usc.edu). As such, the investigators within the ADNI contributed to the design and implementation of ADNI and/or provided data but did not participate in analysis or writing of this report. A complete listing of ADNI investigators can be found at: http://adni.loni.usc.edu/wp-content/uploads/how_to_apply/ADNI_Acknowledgement_List.pdf

² Data used in preparation of this article were obtained from the Frontotemporal Lobar Degeneration Neuroimaging Initiative (FTLDNI) database (<http://4rtini-ftldni.ini.usc.edu/>). The investigators at NIFD/FTLDNI contributed to the design and implementation of FTLDNI and/or provided data but did not participate in analysis or writing of this report.

of neurodegenerative processes (Lee et al., 2016). First, WMHs have a higher prevalence in neurodegenerative diseases such as Alzheimer's disease (AD) (Dadar et al., 2017b; Dubois et al., 2014; Tosto et al., 2014), dementia with Lewy bodies (DLB) (Barber et al., 1999), Parkinson's disease (PD) (Mak et al., 2015; Piccini et al., 1995), frontotemporal dementia (FTD) (Varma et al., 2002), as well as individuals with mild cognitive impairment (MCI) due to AD (DeCarli et al., 2001; Lopez et al., 2003; Dadar et al., 2017b). Second, patients with WMHs present with significantly more severe cognitive deficits and suffer greater future cognitive decline compared with individuals with the same level of neurodegeneration related pathologies without WMHs (Au et al., 2006; Carmichael et al., 2010; Prins and Scheltens, 2015; Dadar et al., 2020b, 2019, 2020a, 2018b).

Few studies have investigated the relationships between longitudinal changes in WMHs, neurodegenerative changes, and cognitive decline. Further, most studies do not factor the WMH distribution by WM anatomical tracts. Burton et al., reported significantly greater total load of WMHs in AD, but not PD or DLB (Burton et al., 2006). In a community-based cohort of 519 older adults, Rizvi et al., found that increased WMH load in association and projection tracts were related to worse memory function (Rizvi et al., 2020). Similarly, Habes et al., reported that WMHs in most tracts were related to age-related atrophy patterns (Habes et al., 2018). Separating the amnesic and non-amnesic MCI patients from the ADNI cohort, Bangen et al., found that non-amnesic MCI participants showed greater occipital WMH volumes relative to the amnesic MCI group. Further, amnesic MCI participants showed greater temporal and occipital WMHs relative to the controls whereas non-amnesic MCI participants had greater frontal, temporal, parietal, and occipital WMHs. Greater WMH in temporal and occipital regions was also associated with faster decline in everyday functioning, with temporal lobe WMHs disproportionately associated with accelerated decline among the non-amnesic MCI (Bangen et al., 2020). In a cohort of 51 healthy controls, 35 subjects with MCI, and 30 AD patients from tertiary neurology centers in Singapore, Vipin et al., showed higher WMH loads in AD, as well as a significant association between WMH burden (particularly for frontal and parietal lobe WMHs) and GM atrophy in MCI. They also reported a significant association between parietal WMH load and global cognition in their MCI cohort (Vipin et al., 2018).

In a sample comprising 359 participants from the Wisconsin Registry for Alzheimer's Prevention (WRAP), Birdsill et al., reported significant associations between lower cognitive speed and flexibility (a component of executive function) and WMH in the superior corona radiata (Birdsill et al., 2014). In a large community-based cohort of older individuals ($n = 461$), Jiang et al., reported that poorer performance in global cognition, processing speed and executive function was associated with higher WMH volumes (Jiang et al., 2018).

In a sample of 426 subjects with cerebral small vessel disease, Tuladhar et al., found that cortical thickness mediated the association between WMH and cognitive performance. Furthermore, they reported associations between WMHs in corpus callosum, internal capsule, corona radiata, posterior thalamic radiation, superior longitudinal fasciculus, and external capsule and lower cortical thickness in frontotemporal regions, as well as associations between WMHs in corpus callosum, corona radiata, posterior thalamic radiation, sagittal stratum, and superior longitudinal fasciculus and greater cortical thickness in paracentral regions (Tuladhar et al., 2015).

In this study, we quantified WMHs in 3 large multi-center cohorts of neurodegenerative diseases, with a total of 1730 subjects and 5774 timepoints (see Table 1). We first investigated the differences between the anatomical distribution of regional WMHs in

AD, PD, FTD, MCI, and cognitively normal individuals. We further investigated the contribution of WMHs to regional GM atrophy and cognitive performance.

2. Methods

2.1. Participants

Data used in this study includes subjects from Alzheimer's Disease Neuroimaging Initiative (ADNI) database (ADNI1/2/GO), the Parkinson's Progression Markers Initiative (PPMI), and the frontotemporal lobar degeneration neuroimaging initiative (FTLDNI) that had T1-weighted and either FLAIR or T2-weighted MR images.

ADNI: The ADNI (adni.loni.usc.edu) was launched in 2003 as a public-private partnership led by Principal Investigator Michael W. Weiner, MD. The primary goal of ADNI has been to test whether serial MRI, positron emission tomography, other biological markers, and clinical and neuropsychological assessment can be combined to measure the progression of MCI and early AD. Data from 1079 ADNI participants ($N_{\text{Control}} = 316$, $N_{\text{MCI}} = 551$, $N_{\text{AD}} = 212$) and 4240 timepoints ($N_{\text{Control}} = 1275$, $N_{\text{MCI}} = 1954$, $N_{\text{AD}} = 1011$) were included in this study.

PPMI: The PPMI (<http://www.ppmi-info.org>) is a longitudinal multi-site clinical study of approximately 600 de novo PD patients and 200 age-matched healthy controls followed over the course of five years. Data from 406 PPMI participants ($N_{\text{Control}} = 135$, $N_{\text{PD}} = 271$) and 820 timepoints ($N_{\text{Control}} = 236$, $N_{\text{PD}} = 584$) were included in this study.

NIFD: The frontotemporal lobar degeneration neuroimaging initiative (FTLDNI) is founded through the National Institute of Aging and started in 2010 (<http://memory.ucsf.edu/research/studies/nifd>). The primary goals of FTLDNI are to identify neuroimaging modalities and methods of analysis for tracking frontotemporal lobar degeneration (FTLD) and to assess the value of imaging versus other biomarkers in diagnostic roles. Data from 245 FTLDNI participants ($N_{\text{Control}} = 120$, $N_{\text{FTD}} = 125$) and 714 timepoints ($N_{\text{Control}} = 370$, $N_{\text{FTD}} = 344$) were included in this study.

Note that while MRI acquisition protocols were similar across studies (specifically, PPMI guidelines suggested use of similar protocols to those of the ADNI), they were not necessarily harmonized between the three studies. For details on MRI acquisition protocols and scanner information, please refer to (<http://adni.loni.usc.edu/methods/mri-tool/mri-acquisition/>, <http://adni.loni.usc.edu/methods/documents/mri-protocols/>) for ADNI, (<https://www.ppmi-info.org/study-design/research-documents-and-sops/>, https://www.ppmi-info.org/sites/default/files/docs/PPMI2.0_002_MRI_TOM_Final_v3.0_20210727.pdf) for PPMI, and (<https://cind.ucsf.edu/research/grants/frontotemporal-lobar-degeneration-neuroimaging-initiative-0>, <https://cind.ucsf.edu/resources/mri-center/standard-image-protocol>) for FTLDNI.

3. Measurements

3.1. GM Atrophy

All the preprocessed and linearly registered (9 parameter registration: 3 translations, 3 rotations, and 3 scaling parameters) T1-weighted images were nonlinearly registered to the MNI-ICBM152-2009c template using the symmetric diffeomorphic image registration (SyN) tool from ANTS (Avants et al., 2009), resulting in a deformation field sampled on a 1 mm^3 grid for each subject/timepoint. Deformation-based morphology (DBM) (Ashburner et al., 1998) maps were calculated by computing the Jacobian determinant of the deformation fields obtained

Table 1
Descriptive statistics for the participants enrolled in this study at baseline. Data are number of participants in each category (N), and mean \pm standard deviation of the variables.

Study	ADNI			PPMI		NIFD	
	NC	MCI	AD	NC	PD	NC	FTD
N _{Participants}	316	551	212	135	271	120	125
N _{Timepoints}	1275	1954	1011	236	584	370	344
Follow-up (ys)	2.57	2.34	1.02	0.49	0.73	2.45	1.06
N _{Female}	138	200	95	40	85	51	73
Age (ys)	74.91 \pm 5.77 ^a	73.35 \pm 7.63 ^a	74.54 \pm 7.75	59.50 \pm 11.70	60.76 \pm 9.46	63.95 \pm 7.56	63.52 \pm 7.03
Education (ys)	16.26 \pm 2.78 ^b	15.90 \pm 2.92 ^c	15.20 \pm 2.96 ^{cb}	16.21 \pm 2.82	15.51 \pm 3.02	17.62 \pm 1.87	16.26 \pm 3.15
ADAS13	9.56 \pm 4.44 ^{ba}	18.52 \pm 6.68 ^{ac}	28.75 \pm 6.90 ^{cb}	-	-	-	-
MoCA	25.85 \pm 2.46 ^{ba}	23.64 \pm 3.19 ^{ac}	17.69 \pm 4.64 ^{cb}	28.34 \pm 1.15 ^d	27.32 \pm 2.29 ^d	27.90 \pm 1.59 ^e	19.19 \pm 6.06 ^e

ADNI, Alzheimer's Disease Neuroimaging Initiative; PPMI, the Parkinson's Progression Markers Initiative;

ADAS, Alzheimer's Disease Assessment Scale; MoCA, the Montreal cognitive assessment score; NC, Normal Control; MCI, Mild Cognitive Impairment; AD=Alzheimer's Dementia; PD, Parkinson's Disease; FTD, Fronto-Temporal Dementia.

^a P_{NC vs. MCI} < 0.05,

^b P_{NC vs. AD} < 0.05,

^c P_{AD vs. MCI} < 0.05,

^d P_{PD vs. NC} < 0.05,

^e P_{PD vs. NC} < 0.05

from these nonlinear transformations, as a proxy of the relative local volume difference between the individual and MNI-ICBM152-2009c template. CerebrA atlas was used to calculate average regional GM volume in 85 cortical and subcortical regions (Manera et al., 2020, 2019).

3.2. WMHs

All T1-weighted, T2-weighted, proton density (PD), and FLAIR MRI scans were preprocessed as previously described, including the following steps: image denoising, intensity inhomogeneity correction, and intensity normalization into range [0 -100] (Dadar et al., 2017c, 2017a). For each subject, the T2-weighted, PD, and FLAIR scans were then co-registered to the T1-weighted scan of the same visit, using a rigid body registration (6 parameters: 3 translations and 3 rotations) with a mutual information cost function (Dadar et al., 2018a). Using a previously validated WMH segmentation method, the WMHs were automatically segmented for all longitudinal visits, using the preprocessed and co-registered scans (Dadar et al., 2017c). The quality of the registrations and segmentations was visually assessed, and the results that did not pass this quality control were excluded ($n = 102$ out of 5774 time-points). Using the WM tracts atlas by Yeh et al., derived from diffusion MRI data of 842 young healthy individuals from the human connectome project (<https://db.humanconnectome.org/>), the WMH volume in 80 WM tracts were calculated by multiplying the WMH mask of each individual (and each timepoint) with each WM tract mask provided by Yeh et al., and calculating the volume of overlapping voxels (in mm³) (Yeh et al., 2018). To achieve this, the WMH masks were first nonlinearly registered to the MNI-ICBM152-2009c average template by applying the nonlinear transformations calculated using the symmetric diffeomorphic image registration (SyN) tool from ANTS (the same transformations used for DBM analyses, detailed in the previous section) (Avants et al., 2009). The WM tract atlas of Yeh et al., (Yeh et al., 2018) resides in the MNI-ICBM152-2009c space. The WMH tract volumes were then log transformed to achieve a normal distribution. To avoid computing regressions in tracts with little WMH data, regions that had no WMH voxels in more than 80% of the subjects were discarded, leaving 45 WM tracts with some WMHs in at least 20% of the population. Table S1 in the supplementary materials lists the WM tracts that were discarded from the analyses. Note that all WMH segmentations were performed consistently using the same technique (Dadar et al., 2017c).

3.3. Cognitive performance

The Alzheimer's Disease (AD) Assessment Scale-Cognitive Subscale (ADAS13) scores were used to assess cognitive performance for the ADNI subjects, and the Montreal Cognitive Assessment (MoCA) scores were used as the cognitive scores of interest for the NIFD and PPMI subjects (no single cognitive score was consistently available for all datasets). In each study, the cognitive performance of the disease cohort was compared against the control group from the same study.

4. Statistical analysis

Longitudinal mixed-effects models were used to assess the differences between MCI, AD, FTD, and PD cohorts and their age-matched normal controls in each population, in 1) WMH burden in each WM tract, 2) average DBM value in each CerebrA GM region, 3) the relationship between regional (anatomical) WM tract WMH loads and regional GM changes, and 4) the relationship between WMHs and cognitive performance. To ensure that the characteristics of the control subjects and patients have been appropriately matched and there is no recruitment-specific difference between the patients and controls, each patient cohort was compared against the matched controls from the same study.

4.1. Differences in anatomical distribution of WMHs between disease groups

To assess whether the patients with MCI, AD, PD, and FTD have significantly higher regional WMH loads (compared with the respective study matched controls), the following mixed-effects models were tested in each of the 45 WM tracts:

$$\text{Regional WMH load} \sim 1 + \text{Cohort} + \text{Age} + \text{Sex} + (1|\text{Subject}) \quad (1)$$

A similar model was used to assess regional GM differences across each cohort (compared with the matched controls) in each of the GM regions:

$$\text{Regional GM volume} \sim 1 + \text{Cohort} + \text{Age} + \text{Sex} + (1|\text{Subject}) \quad (2)$$

The variable of interest in Eq. 1 and Eq. 2 was Cohort, reflecting the differences between the patients and the appropriate matched controls.

4.2. Relationship between WMHs, GM atrophy and cognitive decline

The relationship between regional GM DBM values and regional WMH burden was assessed using the following model for each possible combination of the GM regions and the WM tracts:

$$\begin{aligned} \text{Regional GM volume} &\sim 1 + \text{Regional WMH load} + \text{Cohort} \\ &+ \text{Regional WMH load} : \text{Cohort} + \text{Age} + \text{Sex} + (1|\text{Subject}) \quad (3) \end{aligned}$$

The relationship between regional WMH loads and cognition was assessed through the following models for all tracts and regions:

$$\begin{aligned} \text{Cognitive Score} &\sim 1 + \text{Regional WMH load} + \text{Cohort} \\ &+ \text{Regional WMH load} : \text{Cohort} + \text{Age} + \text{Sex} + (1|\text{Subject}) \quad (4) \end{aligned}$$

The variable of interest in Eq. 3 was the interaction between regional WMH load and Cohort (i.e. *Regional WMH load:Cohort*), reflecting the additional contribution of WMH burden to GM atrophy (compared with the matched controls). Similarly, the variables of interest in Eq. 4 was *Regional WMH load:Cohort*, reflecting the additional contribution of WMHs to cognitive performance in each cohort. ADAS13 was used as the cognitive score of interest for the ADNI subjects (i.e. MCI and AD cohorts), and MoCA was used for the NIFD and PPMI subjects (no single cognitive score was available for all datasets as MoCA was available only for ADNI2 subjects).

Age was considered as a continuous fixed variable. Sex and Cohort were considered as categorical fixed variables. Subject was considered as a categorical random effect. All continuous variables were z-scored in all the analyses.

4.3. Multiple comparison correction

There were 45 comparisons completed for Eq. 1 and Eq. 4, 85 comparisons for Eq. 2, and 45×85 comparisons completed for Eq. 3. All *p* values are reported after correction for multiple comparisons using false discovery rate (FDR) controlling method with a significance threshold of 0.05. All statistical analyses were performed using MATLAB version 2021a.

5. Results

5.1. Demographics

Table 1 provides a summary of the descriptive characteristics for the participants included in this study.

5.2. Differences in anatomical distribution of WMHs between disease groups

Fig. 1 shows the significant differences between WMH burden in each tract (after FDR correction for number of tracts) for each cohort with respect to their study-specific age- and sex-matched normal controls (variable *Cohort* in Eq. 1, i.e., the amount of WMH due to disease). Warmer colors indicate greater WMH burden. A table containing significant t-statistics of the top 20 regional WMH differences between MCI, AD, and FTD cohorts and their corresponding study age-matched controls can be found in Table S2 (Supplementary materials). In the MCI (due to probable AD) cohort, the results show significantly greater WMH burden (in comparison to the matched controls) predominantly in the fornix, anterior commissure, corpus callosum, bilateral cortico-striatal tract and inferior fronto-occipital vertical occipital fasciculi. In the dementia due to probable AD cohort, the results showed significant higher WMH burden for all WM tracts and of greater magnitude compared to MCI subjects, especially in corpus callosum,

fornix, anterior commissure, cortico-striatal and corticothalamic tracts, optic radiations, longitudinal pathways, and parieto-pontine tracts. In the FTD cohort, the results showed higher asymmetric WMH burden with greater involvement of the uncinate fasciculi and cingulum relative to other WM tracts (as a remarkable finding in comparison to MCI and AD), but also significant involvement in fornix, corpus callosum, cortico-striatal and corticothalamic tracts. Of note, increase in WMHs was also present in posterior brain areas. No significant differences were observed in any WM tracts between the de novo PD patients and the PPMI age-matched controls.

Fig. 2 shows the significant differences in GM volumes (after FDR correction) between each cohort and their study-specific age- and sex-matched normal controls (variable *Cohort* in Eq. 2, i.e., the amount of regional GM atrophy due to disease). Colder colors indicate significant shrinkage of the area compared with the ICBM-MNI152-2009c template, i.e. presence of regional atrophy. Note that since age and sex are integrated into the model, these maps show the volume differences over and above what is expected for age (and sex). Table S3 in the Supplementary materials shows t-statistics for the top 20 GM regions with greater atrophy for MCI, AD, FTD, PD cohorts compared to their corresponding study age-matched controls. The MCI cohort showed greater involvement of pericalcarine, entorhinal, pars triangularis, precuneus, cuneus, insula and paracentral regions (Fig. 2, first row). The AD cohort had a diffuse pattern of atrophy with greater involvement of pars triangularis, pericalcarine cortex, bilateral insula, superior and rostral anterior gyri along with asymmetric entorhinal and superior temporal atrophy (Fig. 2, second row). The FTD cohort presented with extensive levels of atrophy, more remarkable in the cingulate, deep nuclei (thalamus and putamen) and cortical areas in the frontal and temporal lobes bilaterally (Fig. 2, third row). The de novo PD cohort had much more limited regions of atrophy, showing only significantly greater bilateral atrophy in the pericalcarine and posterior cingulate areas (Fig. 2, last row).

5.3. Relationship between WMHs, GM atrophy and cognitive decline

Fig. 3 shows the significant interactions between regional WMH load and Cohort (i.e. *Regional WMH load:Cohort* in Eq. 3), reflecting the additional contribution of WMH burden to GM atrophy (compared with the matched controls) in that region (FDR corrected $p < 0.05$). This corresponds to the amount of GM atrophy over and above that due to disease shown in Fig. 2, to query if regional WMH have different damaging effects on the pattern of GM atrophy. In the MCI cohort, bilateral atrophy in the fronto-insular regions (i.e., insula, superior frontal gyrus, lateral orbitofrontal, rostral anterior cingulate and pars triangularis) were associated with greater WMH loads in the anterior commissure, corpus callosum, the cortico-striatal, cortico-thalamic, inferior fronto-occipital, middle longitudinal, and inferior longitudinal pathways. Though bilaterally significant, these associations were of greater magnitude for right sided cortical regions. WMH loads on those tracts were also associated with greater GM atrophy in posterior parietal and occipital regions (posterior cingulate, precuneus, cuneus, lateral occipital cortices) as well as temporal gyri and entorhinal regions. The associations between GM atrophy and regional WMH loads in the AD cohort were similar to those for the MCI, though mainly bilateral and of greater magnitude, i.e., higher levels of WMH burden relating to higher levels of GM atrophy. In the FTD cohort, atrophy in frontal regions such as lingual and superior frontal gyri were associated with WMH load in corpus callosum, cortico-striatal and cortico-thalamic tracts, whereas basal ganglia and posterior cingulate was associated predominantly with WMHs in corpus callosum, corticothalamic, cortico-striatal, frontal aslant and fronto-pontine tracts and in lesser degree with longitudinal fasciculi.

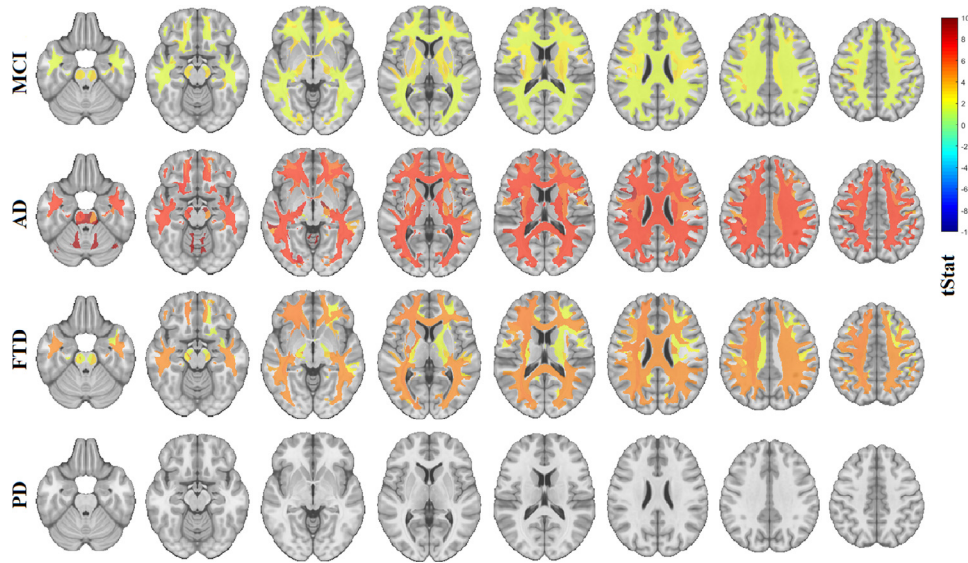


Fig. 1. Regional WMH differences between MCI, AD, FTD, PD cohorts and their corresponding study age-matched controls. Each row includes different axial slices covering the brain, showing the t-statistics for regions that were significantly different between controls and patients after FDR correction. WMH= white matter hyperintensities. MCI, mild cognitive impairment; AD, Alzheimer's dementia; FTD, fronto-temporal dementia; PD, Parkinson's disease; Images presented in neurological format, i.e. left is on left. (Color version of figure is available online).

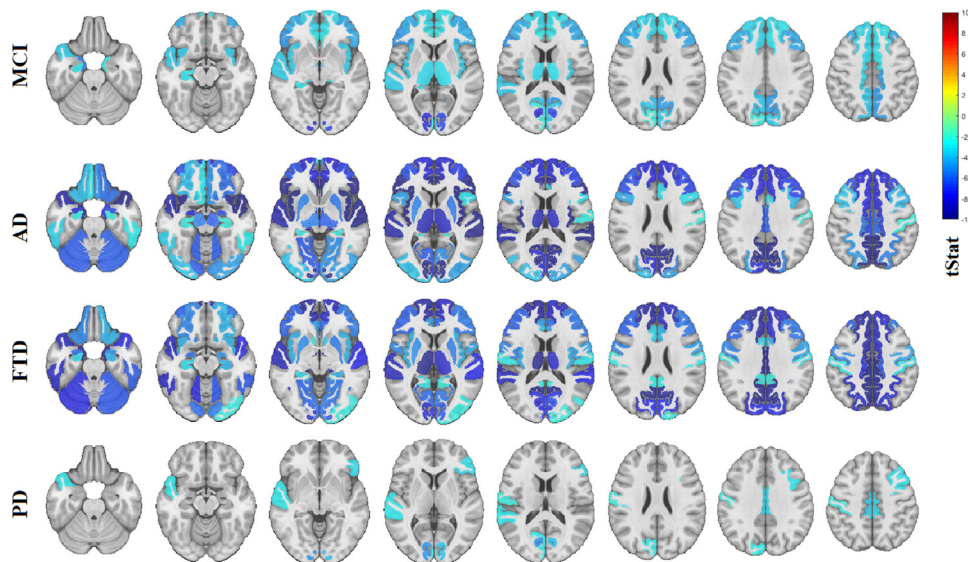


Fig. 2. Regional grey matter differences between MCI, AD, FTD, PD cohorts and their age-matched controls. Each row includes different axial slices covering the brain, showing the t-statistics for regions that were significantly different between controls and patients after FDR correction. MCI, mild cognitive impairment; AD, Alzheimer's dementia; FTD, fronto-temporal dementia; PD, Parkinson's disease; Images presented in neurological format. (Color version of figure is available online).

Fig. 4 shows the significant interactions between cohort and WMH burden (i.e., the term *Regional WMH load:Cohort* in Eq. 4) in each of the WM tracts affecting cognition, indicating the *additional* contribution of WMH burden to cognitive deficits, compared with the matched controls for each cohort (FDR corrected $p < 0.05$). WMHs in most tracts contributed to greater cognitive deficits in AD and FTD, whereas their impact on cognitive performance in MCI and PD cohorts were not significantly different from their impact on the matched controls. The magnitude of this additional contribution of WMH to cognitive impairment and the extension of WM tracts involved was greater for AD than FTD. A table containing the t-statistic values for the top 20 significant interactions between cohort and WMH loads per tract affecting cognitive scores can be found in Table S4 in the Supplementary materials.

6. Discussion

In this study, we combined data from three publicly available large databases to investigate the prevalence of regional WMHs in WM tracts and regional GM atrophy, as well as their interplay and impact on cognitive function in 3 neurodegenerative diseases; namely AD, FTD, and PD. Our results showed significantly greater WMH burden in MCI, AD, and FTD patients, compared with the matched controls, but not in the PD cohort. These findings are in line with previous studies, showing significantly higher WMH loads in MCI (Dadar et al., 2017b; DeCarli et al., 2001; Lopez et al., 2003), AD (Capizzano et al., 2004; Dubois et al., 2014; Tosto et al., 2014), and FTD patients (Huynh et al., 2021; Varma et al., 2002), but not in de novo PD (Dadar et al., 2018b; Dalaker et al., 2009).

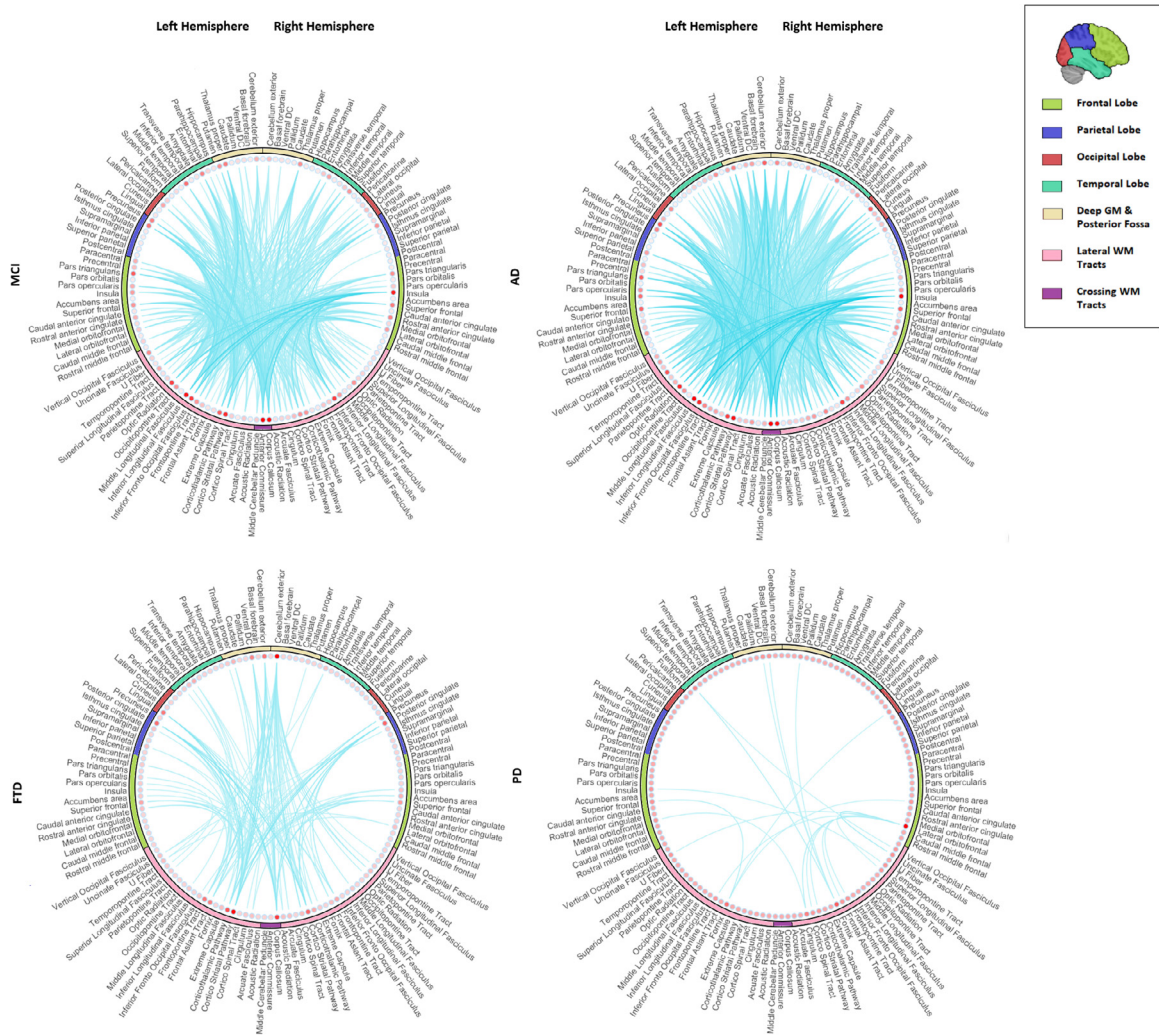


Fig. 3. Significant interactions between WMH loads per tract and cohort, impacting regional GM volumes in MCI, and AD, FTD, and PD patients (Eq. 3). Each blue line represents a statistically significant connection between a WM tract and increased atrophy in a brain (FDR corrected p -value < 0.05). Line intensities indicate t -statistics, with higher intensities indicating higher levels of atrophy (lower DBM values) relating to higher WMH burden. Node intensities (indicated in red) reflect the overall weight of the correlations for each region. WMH, White Matter Hyperintensities; DBM, Deformation Based Morphometry; PD, Parkinson's Disease; FTD, Fronto-temporal Dementia; MCI, Mild Cognitive Impairment; AD, Alzheimer's Dementia. (Color version of figure is available online).

Other studies investigating later stage PD patients do however report higher incidence of WMHs (Mak et al., 2015; Piccini et al., 1995), substantiating the possibility that the increase might occur at later stages of the disease.

We observed significant levels of GM atrophy in regions that are commonly associated with each disease. The MCI cohort had an overall pattern of atrophy mostly in the medial temporal lobes, insula, cuneus and precuneus. The AD cohort presented with greater levels of atrophy in similar regions. The diffuse pattern of atrophy found in AD was consistent with Braak disease progression stages where the neurofibrillary pathology extends to frontal, superolateral, and occipital directions (Braak et al., 2006; Chan et al., 2001; Jucker and Walker, 2013). The FTD cohort presented with extensive levels of atrophy, greater in the deep nuclei, cingulate and cortical areas in frontal and temporal lobes (Cardenas et al., 2007; Landin-Romero et al., 2017; Manera et al., 2019; Whitwell et al., 2015). Finally, the de novo PD cohort had bilateral atrophy significantly greater than controls in the pericalcarine and posterior cingulate regions. Of note, the patterns of GM involvement shown in (Fig 2) overlap significantly between AD and FTD cohorts. This could be in line firstly, with intermediate to advanced stages of the disease for

both as reflected in the cognitive scores (MoCAAD: 17.69 ± 4.64 and MoCAFTD: 19.19 ± 0.06). Secondly, compared to cortical thickness, conventional voxel-based techniques are a less sensitive measurement to detect regional cortical gray matter changes related to neurodegeneration, but they are also less impacted by the presence of WMH which, as shown, are remarkably present in both cohorts. Notwithstanding, a few differences were identified: 1) AD showed more involvement of parieto-occipital regions; 2) we found significant bilateral parietal involvement in FTD, though with a lesser degree of atrophy compared to frontal and temporal structures; 3) the involvement showed by FTD was slightly more asymmetrical than AD. We also observed significant differences in areas not typically associated with the specific diseases, such as significant insular atrophy in the MCI cohort, and occipital atrophy in the AD cohort. While not a feature of the disease, atrophy in the posterior regions of insula has been previously reported, particularly in amnesic MCI patients and has been linked to progression to AD (Davatzikos et al., 2011; Spulber et al., 2012; Xie et al., 2012). Accelerated rate of atrophy in insular regions and occipital lobes have also been reported in AD patients along with the progression of the disease (Sluimer et al., 2009).

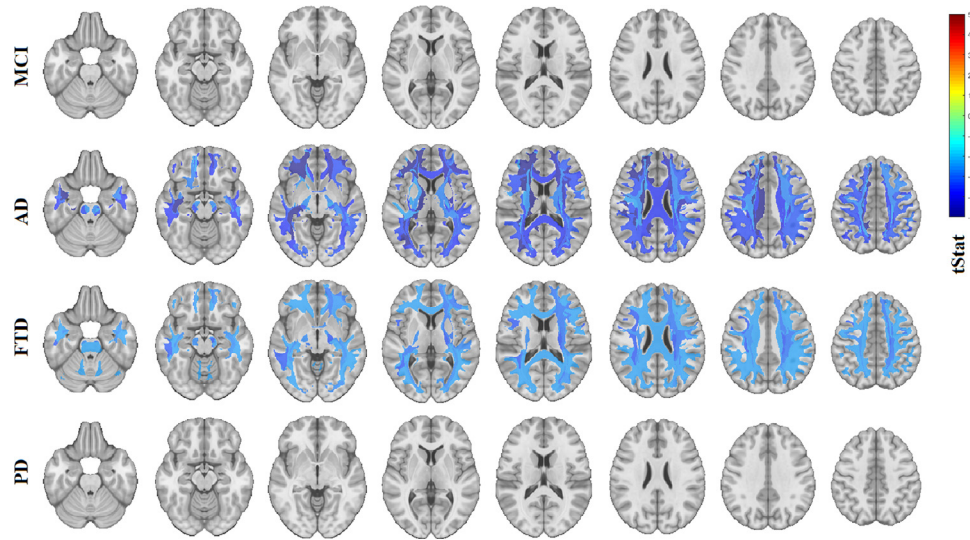


Fig. 4. Significant interactions between cohort and WMH loads per tract affecting cognitive scores in PD, FTD, MCI, and AD patients (FDR corrected p -value < 0.05). Colors indicate the t-statistic values from the mixed effects models (Eq. 4), with colder colors indicating poorer cognitive performance relating to higher WMH burden. WMH, White Matter Hyperintensities; PD, Parkinson's Disease; FTD, Fronto-temporal Dementia; MCI, Mild Cognitive Impairment; AD, Alzheimer's Dementia. All images in neurological format. (Color version of figure is available online).

Previous studies have reported associations between WMH load and GM atrophy in the elderly and AD patients (Dadar et al., 2020a; Wen et al., 2006). Furthermore, other studies have shown the spatial distribution of WMHs and atrophy in AD (Brickman et al., 2012; Yoshita et al., 2006) and FTD (Chao et al., 2007; Huynh et al., 2021) as well as its diagnostic and prognostic relevance. The extent and progression of WM involvement has also been related to greater cortical thinning in PD (Foo et al., 2016). However, to our knowledge, no previous studies had investigated the association between WMH loads in different WM tracts with GM atrophy in different neurodegenerative diseases. In the present study, we found that WMH loads in WM tracts were associated with GM atrophy in regions connected to those tracts, corresponding to the patterns of atrophy characteristic of each disease. This might indicate a specific contribution of the cerebrovascular pathology (or other aetiologies reflected in the MRI as WMHs) to the disease-specific patterns of atrophy, as opposed to a nonspecific additional factor that would have been associated with atrophy over all brain regions. Specifically, high WMH burden can be observed in FTD patients in absence of significant vascular risk factors and pathology, possibly due to other pathological processes related to certain genetic mutations (Caroppo et al., 2014; Desmarais et al., 2021; Sudre et al., 2019; Woollacott et al., 2018). Unfortunately, our FTD sample is derived from a mainly sporadic cohort (FTLDNI), limiting our ability to investigate whether the FTD patients were carriers of specific mutations, previously linked to increased WMH burden in genetic forms of FTD (Caroppo et al., 2014; Desmarais et al., 2021; Sudre et al., 2019; Woollacott et al., 2018). In a recent study, Desmarais et al. reported presence of severe gliosis, myelin pallor, and axonal loss in 15 AD and 58 FTD cases with severe WMH burden, but with no distinguishing features indicative of the underlying proteinopathy. Vascular pathology in the form of venous collagenosis was also reported, but no cases showed arteriolosclerosis, infarction, or perivascular hemosiderin (Desmarais et al., 2021). Further investigations using post-mortem histopathology assessment data are necessary to determine the underlying pathology of these WMHs.

In the present study, significant interactions between WMH load and disease groups have been found for many brain regions, reflecting the additional contribution of WMH burden to GM at-

rophy in that region above and beyond the effect expected for the disease by itself. (Fig. 3). In general, for MCI and AD cohorts, WMH load in the anterior commissure, corpus callosum, the cortico-striatal, cortico-thalamic and inferior longitudinal pathways was associated with greater GM atrophy in the insula, posterior cingulate, superior frontal and entorhinal regions. In the FTD cohort, WMHs in corpus callosum, cortico-thalamic, cortico-striatal, frontal aslant and fronto-pontine tracts showed significant interactions with atrophy in frontal regions (i.e., lingual, and superior frontal gyri) as well as atrophy in the basal ganglia. Fig. 3 shows the associations between WMH loads and additional GM atrophy in each cohort, and not connectivity. Therefore, due to the high correlation of the corresponding WMH loads in left and right WM tracts, some of the associations were also found between cortical regions on one hemisphere and the association or projection tracts on the other hemisphere, though generally with lower t-statistics values.

WMH burden in most tracts contributed to greater cognitive deficits in the dementia cohorts (i.e. AD and FTD), whereas their impact on cognitive performance in MCI and PD cohorts were not significantly different from their impact on the matched controls. In other words, in AD and FTD, a certain amount of WMHs might have a more negative impact on cognition than in controls, suggesting a synergy between these proteinopathies and cerebrovascular disease. These findings are also in line with previous studies reporting greater WMH-related cognitive deficits in AD and FTD (Au et al., 2006; Carmichael et al., 2010; Dadar et al., 2019, 2018b; Prins and Scheltens, 2015). As for PD, while some studies did not find any association between WM measures and change in cognitive scores (Burton et al., 2006), Foo et al., found that progression in WM involvement was associated not only with greater cortical thinning but also with domain specific cognitive impairment (Foo et al., 2016). However, their PD cohort (mild PD patients) had a longer average disease duration (~ 4.7 years at baseline) than the de novo patients studied here (~ 0.6 years at baseline). Similarly, in a previous study in the same cohort (Dadar et al., 2018b), while we did not find an association between baseline WMHs and baseline cognitive status (all PD patients were cognitively normal at baseline), using longitudinal cognitive data (mean follow-up duration = 4.09 years), we found that whole brain WMH loads at

baseline were associated with greater future cognitive decline in the PD patients. However, since those longitudinal follow-up visits did not have accompanying MRI data (only a subset of the population was longitudinally scanned, whereas cognitive assessment was performed longitudinally for all participants), after correction for multiple comparisons, we did not find significant associations between tract specific WMH loads and cognition in the de novo PD cohort.

One major limitation of the present study was the inconsistencies between the three datasets used. While the MRI acquisition protocols were similar across studies (i.e. PPMI guidelines suggested use of ADNI protocols), they were not necessarily harmonized between the 3 datasets. Another important difference was in the follow up duration and the number of follow up visits between the different studies (mean number of follow up visits $N_{ADNI}=3.8$, $N_{NIFD}=2.6$, and $N_{PPMI}=1.6$). In addition, there was no single cognitive score that was available for all three datasets (ADNI1 subjects did not have MoCA assessments, whereas PPMI and NIFD subjects did not have ADAS assessments). To ensure that these differences, as well as any differences in subject inclusion and exclusion criteria did not impact the results, each analysis was performed using matched controls from the same study.

Another limitation was the use of the PPMI dataset, which only includes de novo PD patients, all of which were cognitively normal at baseline. While this allows us to establish the earliest disease related changes, lack of later stage PD patients (i.e. PD patients with dementia) might have prevented us from assessing the full spectrum of both GM and WM changes and their interplay and impact on cognition in PD (Foo et al., 2016). Future studies in populations including later stage PD patients are necessary to establish such associations.

Due to sample size and statistical power limitations (i.e. correcting for 45, 85, and 45*85 multiple comparisons for models from Eq. 1 – 3, respectively), we did not investigate potential differences between specific subtypes in each diagnostic group; such as stable versus progressive or amnesic versus non-amnesic in the MCI group, and behavioural versus language variants in the FTD group. Further investigations in datasets with larger sample sizes are therefore warranted to assess such differences.

It is important to note that all the image processing, registration, and segmentation pipelines used in this study have been developed and extensively validated for use in multi-center and multi-scanner settings, and have since been successfully applied to various multi-center studies of aging and neurodegenerative disease populations (Anor et al., 2021; Dadar et al., 2020c; Dadar and Duchesne, 2020; Manera et al., 2021; Sanford et al., 2019), including the cohorts used in the current study (Dadar et al., 2021, 2020a, 2019; Manera et al., 2019; Misquitta et al., 2020; Zeighami et al., 2019, 2015). We did not include scanner information or education as covariates in our main models, since not all studies had this information available for all the participants. However, to ensure that such differences do not impact the findings of our study, we repeated the analyses with these variables included in the models (site ID as a categorical random effect and education as a continuous fixed effect) for the studies that did have the information available, and obtained results similar to those reported.

In conclusion, WMHs occur more extensively in AD, MCI and FTD patients than age-matched normal controls. WMH burden on WM tracts also correlates with regional GM atrophy in pathologically relevant areas (i.e. the frontal lobe for FTD, and diffuse but mainly parietal and temporal lobes for AD). Subjects with AD and FTD are also more sensitive to the negative cognitive effect of WMHs compared to controls. This suggests a potentially synergistic involvement of cerebrovascular disease in these specific pathologies, as opposed to a simple comorbid process. This un-

derlines the need for further longitudinal investigations into the impact of WMHs in neurodegenerative diseases and its impact on treatment efficacy in clinical trials. Clinicians should view WMHs as an intrinsic part of the dementia process and should be targeted with aggressive strategy based on primary and secondary prevention of vascular risk factors (anti-hypertensive medications, blood sugar management, lipid-lowering treatment, exercise, and lifestyle changes), which might slow down progression of WM damage and potentially slow down cognitive decline in neurodegenerative diseases (DeBette and Markus, 2010).

Author contributions

Mahsa Dadar: Conceptualization, Formal analysis, Methodology, Visualization, Writing - original draft, Writing - review & editing.

Ana L. Manera: Conceptualization, Interpretation of findings, Writing - review & editing.

Simon Ducharme: Conceptualization, Supervision, Writing - review & editing.

D. Louis Collins: Conceptualization, Supervision, Writing - review & editing.

Disclosure statement

The authors declare no competing interests.

Acknowledgements

We would like to acknowledge funding from the Famille Louise & André Charron. MD is supported by a scholarship from the Canadian Consortium on Neurodegeneration in Aging in which DLC is a co-investigator as well as an Alzheimer Society Research Program (ASRP) postdoctoral award. The Consortium is supported by a grant from the Canadian Institutes of Health Research with funding from several partners including the Alzheimer Society of Canada, Sanofi, and Women's Brain Health Initiative.

Data collection and sharing for this project was in part funded by the Alzheimer's Disease Neuroimaging Initiative (ADNI) (National Institutes of Health Grant U01 AG024904) and DOD ADNI (Department of Defense award number W81XWH-12-2-0012). ADNI is funded by the National Institute on Aging, the National Institute of Biomedical Imaging and Bioengineering, and through generous contributions from the following: AbbVie, Alzheimer's Association; Alzheimer's Drug Discovery Foundation; Araclon Biotech; BioClinica, Inc.; Biogen; Bristol-Myers Squibb Company; CereSpir, Inc.; Cogstate; Eisai Inc.; Elan Pharmaceuticals, Inc.; Eli Lilly and Company; EuroImmun; F. Hoffmann-La Roche Ltd and its affiliated company Genentech, Inc.; Fujirebio; GE Healthcare; IXICO Ltd.; Janssen Alzheimer Immunotherapy Research & Development, LLC.; Johnson & Johnson Pharmaceutical Research & Development LLC.; Lumosity; Lundbeck; Merck & Co., Inc.; Meso Scale Diagnostics, LLC.; NeuroRx Research; Neurotrack Technologies; Novartis Pharmaceuticals Corporation; Pfizer Inc.; Piramal Imaging; Servier; Takeda Pharmaceutical Company; and Transition Therapeutics. The Canadian Institutes of Health Research is providing funds to support ADNI clinical sites in Canada. Private sector contributions are facilitated by the Foundation for the National Institutes of Health (www.fnih.org). The grantee organization is the Northern California Institute for Research and Education, and the study is coordinated by the Alzheimer's Therapeutic Research Institute at the University of Southern California. ADNI data are disseminated by the Laboratory for Neuro Imaging at the University of Southern California.

Data collection and sharing for this project was in part funded by the Frontotemporal Lobar Degeneration Neuroimaging Initia-

tive (National Institutes of Health Grant R01 AG032306). The study is coordinated through the University of California, San Francisco, Memory and Aging Center. FTLDNI data are disseminated by the Laboratory for Neuro Imaging at the University of Southern California.

Data used in this article were in part obtained from the Parkinson's Progression Markers Initiative (PPMI) database (www.ppmi-info.org/data). For up-to-date information on the study, visit www.ppmi-info.org. PPMI is sponsored and partially funded by the Michael J Fox Foundation for Parkinson's Research and funding partners, including AbbVie, Avid Radiopharmaceuticals, Biogen, Bristol-Myers Squibb, Covance, GE Healthcare, Genentech, Glaxo-SmithKline (GSK), Eli Lilly and Company, Lundbeck, Merck, Meso Scale Discovery (MSD), Pfizer, Piramal Imaging, Roche, Servier, and UCB (www.ppmi-info.org/fundingpartners).

Supplementary materials

Supplementary material associated with this article can be found, in the online version, at [doi:10.1016/j.neurobiolaging.2021.11.007](https://doi.org/10.1016/j.neurobiolaging.2021.11.007).

References

Abraham, H.M.A., Wolfson, L., Moscufo, N., Guttman, C.R., Kaplan, R.F., White, W.B., 2016. Cardiovascular risk factors and small vessel disease of the brain: blood pressure, white matter lesions, and functional decline in older persons. *J. Cereb. Blood Flow Metab* 36, 132–142.

Anor, C.J., Dadar, M., Collins, D.L., Tartaglia, M.C., 2021. The longitudinal assessment of neuropsychiatric symptoms in mild cognitive impairment and Alzheimer's disease and their association with white matter hyperintensities in the national alzheimer's coordinating center's uniform data set. *Biol. Psychiatry Cogn. Neurosci. Neuroimaging, Imaging Biomarkers and Outcome Prediction* 6, 70–78. [doi:10.1016/j.bpsc.2020.03.006](https://doi.org/10.1016/j.bpsc.2020.03.006).

Ashburner, J., Hutton, C., Frackowiak, R., Johnsrude, I., Price, C., Friston, K., 1998. Identifying global anatomical differences: deformation-based morphometry. *Hum. Brain Mapp* 6, 348–357. [doi:10.1002/\(SICI\)1097-0193\(1998\)6:5/6<348::AID-HBM4>3.0.CO;2-P](https://doi.org/10.1002/(SICI)1097-0193(1998)6:5/6<348::AID-HBM4>3.0.CO;2-P).

Au, R., Massaro, J.M., Wolf, P.A., Young, M.E., Beiser, A., Seshadri, S., D'Agostino, R.B., DeCarli, C., 2006. Association of white matter hyperintensity volume with decreased cognitive functioning: the framingham heart study. *Arch. Neurol* 63, 246–250.

Avants, B.B., Tustison, N., Song, G., 2009. Advanced normalization tools (ANTS). *Insight, J* 2, 1–35.

Bangen, K.J., Thomas, K.R., Weigand, A.J., Sanchez, D.L., Delano-Wood, L., Edmonds, E.C., Carmichael, O.T., Schwarz, C.G., Brickman, A.M., Bondi, M.W., 2020. Pattern of regional white matter hyperintensity volume in mild cognitive impairment subtypes and associations with decline in daily functioning. *Neurobiol. Aging* 86, 134–142. [doi:10.1016/j.neurobiolaging.2019.10.016](https://doi.org/10.1016/j.neurobiolaging.2019.10.016).

Barber, R., Scheltens, P., Gholkar, A., Ballard, C., McKeith, I., Ince, P., Perry, R., O'Brien, J., 1999. White matter lesions on magnetic resonance imaging in dementia with Lewy bodies, Alzheimer's disease, vascular dementia, and normal aging. *J. Neurol. Neurosurg. Psychiatry* 67, 66–72. [doi:10.1136/jnnp.67.1.66](https://doi.org/10.1136/jnnp.67.1.66).

Birdsill, A.C., Kosick, R.L., Jonaitis, E.M., Johnson, S.C., Okonkwo, O.C., Hermann, B.P., LaRue, A., Sager, M.A., Bendlin, B.B., 2014. Regional white matter hyperintensities: aging, Alzheimer's disease risk, and cognitive function. *Neurobiol. Aging* 35, 769–776. [doi:10.1016/j.neurobiolaging.2013.10.072](https://doi.org/10.1016/j.neurobiolaging.2013.10.072).

Braak, H., Alafuzoff, I., Arzberger, T., Kretschmar, H., Del Tredici, K., 2006. Staging of Alzheimer disease-associated neurofibrillary pathology using paraffin sections and immunocytochemistry. *Acta Neuropathol. (Berl.)* 112, 389–404.

Brickman, A.M., Provenzano, F.A., Muraskin, J., Manly, J.J., Blum, S., Apa, Z., Stern, Y., Brown, T.R., Luchsinger, J.A., Mayeux, R., 2012. Regional white matter hyperintensity volume, not hippocampal atrophy, predicts incident Alzheimer disease in the community. *Arch. Neurol* 69, 1621–1627.

Burton, E.J., McKeith, I.G., Burn, D.J., Firbank, M.J., O'Brien, J.T., 2006. Progression of white matter hyperintensities in Alzheimer Disease, dementia with lewy bodies, and parkinson disease dementia: a comparison with normal aging. *Am. J. Geriatr. Psychiatry* 14, 842–849. [doi:10.1097/01.JGP.0000236596.56982.1c](https://doi.org/10.1097/01.JGP.0000236596.56982.1c).

Capizzano, A.A., Ación, L., Bekinschtein, T., Furman, M., Gomila, H., Martínez, A., Mizrahi, R., Starkstein, S.E., 2004. White matter hyperintensities are significantly associated with cortical atrophy in Alzheimer's disease. *J. Neurol. Neurosurg. Psychiatry* 75, 822–827. [doi:10.1136/jnnp.2003.019273](https://doi.org/10.1136/jnnp.2003.019273).

Cardenas, V.A., Boxer, A.L., Chao, L.L., Gorno-Tempini, M.L., Miller, B.L., Weiner, M.W., Studholme, C., 2007. Deformation-based morphometry reveals brain atrophy in frontotemporal dementia. *Arch. Neurol* 64, 873–877. [doi:10.1001/archneur.64.6.873](https://doi.org/10.1001/archneur.64.6.873).

Carmichael, O., Schwarz, C., Drucker, D., Fletcher, E., Harvey, D., Beckett, L., Jack, C.R., Weiner, M., DeCarli, C., 2010. Longitudinal changes in white matter disease and cognition in the first year of the alzheimer disease neuroimaging initiative. *Arch. Neurol* 67, 1370–1378. [doi:10.1001/archneur.2010.284](https://doi.org/10.1001/archneur.2010.284).

Caroppo, P., Le Ber, I., Camuzat, A., Clot, F., Naccache, L., Lamari, F., De Septenville, A., Bertrand, A., Belliard, S., Hannequin, D., Colliot, O., Brice, A., 2014. Extensive white matter involvement in patients with frontotemporal lobar degeneration: think progranulin. *JAMA Neurol* 71, 1562–1566. [doi:10.1001/jamaneurol.2014.1316](https://doi.org/10.1001/jamaneurol.2014.1316).

Chan, D., Fox, N.C., Jenkins, R., Scahill, R.I., Crum, W.R., Rossor, M.N., 2001. Rates of global and regional cerebral atrophy in AD and frontotemporal dementia. *Neurology* 57, 1756–1763.

Chao, L.L., Schuff, N., Clevenger, E.M., Mueller, S.G., Rosen, H.J., Gorno-Tempini, M.L., Kramer, J.H., Miller, B.L., Weiner, M.W., 2007. Patterns of white matter atrophy in frontotemporal lobar degeneration. *Arch. Neurol* 64, 1619–1624. [doi:10.1001/archneur.64.11.1619](https://doi.org/10.1001/archneur.64.11.1619).

Dadar, M., Ali Pascoal, T., Sarinporn, J., Misquitta, K., Fonov, V.S., Brietner, J., Rosa neto, P., DeCarli, C., Carmichael, O., Collins, D.L., 2017. Validation of a regression technique for segmentation of white matter hyperintensities in Alzheimer's disease. *IEEE Trans. Med. Imaging* 36 (8), 1758–1768. [doi:10.1109/TMI.2017.2693978](https://doi.org/10.1109/TMI.2017.2693978).

Dadar, M., Camicioli, R., Duchesne, S., Collins, D.L., Initiative, A.D.N., 2020a. The temporal relationships between white matter hyperintensities, neurodegeneration, amyloid beta, and cognition. *Alzheimers Dement. Diagn. Assess. Dis. Monit* 12, e12091.

Dadar, M., Duchesne, S., 2020. Reliability assessment of tissue classification algorithms for multi-center and multi-scanner data. *NeuroImage* 217, 116928. [doi:10.1016/j.neuroimage.2020.116928](https://doi.org/10.1016/j.neuroimage.2020.116928).

Dadar, M., Fonov, V.S., Collins, D.L., Initiative, A.D.N., 2018a. A comparison of publicly available linear MRI stereotaxic registration techniques. *NeuroImage* 174, 191–200.

Dadar, M., Gee, M., Shuaib, A., Duchesne, S., Camicioli, R., 2020b. Cognitive and motor correlates of grey and white matter pathology in Parkinson's disease. *NeuroImage* Clin 27, 102353. [doi:10.1016/j.nicl.2020.102353](https://doi.org/10.1016/j.nicl.2020.102353).

Dadar, M., Manera, A.L., Zinman, L., Korngut, L., Genge, A., Graham, S.J., Frayne, R., Collins, D.L., Kalra, S., 2020c. Cerebral atrophy in amyotrophic lateral sclerosis parallels the pathological distribution of TDP43. *Brain Commun* 2, fcaa061.

Dadar, M., Maranzano, J., Ducharme, S., Carmichael, O.T., Decarli, C., Collins, D.L., 2018. Validation of T1w-based segmentations of white matter hyperintensity volumes in large-scale datasets of aging. *Hum. Brain Mapp* 39 (3), 1093–1107.

Dadar, M., Maranzano, J., Ducharme, S., Collins, D.L., 2019. White matter in different regions evolves differently during progression to dementia. *Neurobiol. Aging* 76, 71–79. [doi:10.1016/j.neurobiolaging.2018.12.004](https://doi.org/10.1016/j.neurobiolaging.2018.12.004).

Dadar, M., Maranzano, J., Misquitta, K., Anor, C.J., Fonov, V.S., Tartaglia, M.C., Carmichael, O.T., Decarli, C., Collins, D.L., 2017c. Performance comparison of 10 different classification techniques in segmenting white matter hyperintensities in aging. *NeuroImage* 157, 233–249. [doi:10.1016/j.neuroimage.2017.06.009](https://doi.org/10.1016/j.neuroimage.2017.06.009).

Dadar, M., Potvin, O., Camicioli, R., Duchesne, S., Initiative, A.D.N., 2021. Beware of white matter hyperintensities causing systematic errors in FreeSurfer gray matter segmentations! *Hum. Brain Mapp* 42, 2734–2745.

Dadar, M., Zeighami, Y., Yau, Y., Fereshtehnejad, S.-M., Maranzano, J., Postuma, R.B., Dagher, A., Collins, D.L., 2018b. White matter hyperintensities are linked to future cognitive decline in de novo Parkinson's disease patients. *NeuroImage Clin* 20, 892–900.

Dalaker, T.O., Larsen, J.P., Bergsland, N., Beyer, M.K., Alves, G., Dwyer, M.G., Tysnes, O.-B., Benedict, R.H., Kelemen, A., Bronnick, K., 2009. Brain atrophy and white matter hyperintensities in early Parkinson's disease. *Mov. Disord. Off. J. Mov. Disord. Soc* 24, 2233–2241.

Davatzikos, C., Bhatt, P., Shaw, L.M., Batmanghelich, K.N., Trojanowski, J.Q., 2011. Prediction of MCI to AD conversion, via MRI, CSF biomarkers, and pattern classification. *Neurobiol. Aging* 32, 2322. [doi:10.1016/j.neurobiolaging.2010.05.023](https://doi.org/10.1016/j.neurobiolaging.2010.05.023).

Debette, S., Markus, H.S., 2010. The clinical importance of white matter hyperintensities on brain magnetic resonance imaging: systematic review and meta-analysis. *BMJ* 341, c3666.

DeCarli, C., Miller, B.L., Swan, G.E., Reed, T., Wolf, P.A., Carmelli, D., 2001. Cerebrovascular and brain morphologic correlates of mild cognitive impairment in the national heart, lung, and blood institute twin study. *Arch. Neurol* 58, 643–647.

Desmarais, P., Gao, A.F., Lanctôt, K., Rogaeva, E., Ramirez, J., Herrmann, N., Stuss, D.T., Black, S.E., Keith, J., Masellis, M., 2021. White matter hyperintensities in autopsy-confirmed frontotemporal lobar degeneration and Alzheimer's disease. *Alzheimers Res. Ther* 13, 1–16.

Dubois, B., Feldman, H.H., Jacova, C., Hampel, H., Molinuevo, J.L., Blennow, K., DeKosky, S.T., Gauthier, S., Selkoe, D., Bateman, R., 2014. Advancing research diagnostic criteria for Alzheimer's disease: the IWG-2 criteria. *Lancet Neurol* 13, 614–629.

Foo, H., Mak, E., Yong, T.T., Wen, M.-C., Chander, R.J., Au, W.L., Tan, L., Kandiah, N., 2016. Progression of small vessel disease correlates with cortical thinning in Parkinson's disease. *Parkinsonism Relat. Disord* 31, 34–40. [doi:10.1016/j.parkreldis.2016.06.019](https://doi.org/10.1016/j.parkreldis.2016.06.019).

Gouw, A.A., Seewann, A., Van Der Flier, W.M., Barkhof, F., Rozemuller, A.M., Scheltens, P., Geurts, J.J., 2011. Heterogeneity of small vessel disease: a systematic review of MRI and histopathology correlations. *J. Neurol. Neurosurg. Psychiatry* 82 (2), 126–135.

Habes, M., Erus, G., Toledo, J.B., Bryan, N., Janowitz, D., Doshi, J., Völzke, H., Schminke, U., Hoffmann, W., Grabe, H.J., Wolk, D.A., Davatzikos, C., 2018. Re-

- gional tract-specific white matter hyperintensities are associated with patterns of aging-related brain atrophy via vascular risk factors, but also independently. *Alzheimers Dement. Diagn. Assess. Dis. Monit* 10, 278–284. doi:10.1016/j.dadm.2018.02.002.
- Hachinski, V.C., Potter, P., Merskey, H., 1987. Leuko-Araiosis. *Arch. Neurol* 44, 21–23. doi:10.1001/archneur.1987.00520130013009.
- Huynh, K., Piguet, O., Kwok, J., Dobson-Stone, C., Halliday, G.M., Hodges, J.R., Landin-Romero, R., 2021. Clinical and biological correlates of white matter hyperintensities in patients with behavioral-variant frontotemporal dementia and Alzheimer Disease. *Neurology* 96, e1743–e1754. doi:10.1212/WNL.00000000000011638.
- Jiang, J., Paradise, M., Liu, T., Armstrong, N.J., Zhu, W., Kochan, N.A., Brodaty, H., Sachdev, P.S., Wen, W., 2018. The association of regional white matter lesions with cognition in a community-based cohort of older individuals. *NeuroImage Clin* 19, 14–21. doi:10.1016/j.nicl.2018.03.035.
- Jucker, M., Walker, L.C., 2013. Self-propagation of pathogenic protein aggregates in neurodegenerative diseases. *Nature* 501, 45–51.
- Landin-Romero, R., Kumfor, F., Leyton, C.E., Irish, M., Hodges, J.R., Piguet, O., 2017. Disease-specific patterns of cortical and subcortical degeneration in a longitudinal study of Alzheimer's disease and behavioural-variant frontotemporal dementia. *NeuroImage* 151, 72–80. doi:10.1016/j.neuroimage.2016.03.032.
- Lee, S., Viqar, F., Zimmerman, M.E., Narkhede, A., Tosto, G., Benzinger, T.L.S., Marcus, D.S., Fagan, A.M., Goate, A., Fox, N.C., Cairns, N.J., Holtzman, D.M., Buckles, V., Ghetti, B., McDade, E., Martins, R.N., Saykin, A.J., Masters, C.L., Ringman, J.M., Ryan, N.S., Förster, S., Laske, C., Schofield, P.R., Sperling, R.A., Saloway, S., Correia, S., Jack, C., Weiner, M., Bateman, R.J., Morris, J.C., Mayeux, R., Brickman, A.M., 2016. White matter hyperintensities are a core feature of Alzheimer's disease: evidence from the dominantly inherited Alzheimer network. *Ann. Neurol* 79 (6), 929–939. doi:10.1002/ana.24647.
- Lopez, O.L., Jagust, W.J., DeKosky, S.T., Becker, J.T., Fitzpatrick, A., Dulberg, C., Breitzer, J., Lyketos, C., Jones, B., Kawas, C., 2003. Prevalence and classification of mild cognitive impairment in the cardiovascular health study cognition study: part 1. *Arch. Neurol* 60, 1385–1389.
- Mak, E., Dwyer, M.G., Ramasamy, D.P., Au, W.L., Tan, L., Zivadinov, R., Kandiah, N., 2015. White matter hyperintensities and mild cognitive impairment in Parkinson's disease. *J. Neuroimaging* 25, 754–760.
- Manera, A.L., Dadar, M., Collins, D.L., Ducharme, S., Initiative, F.L.D.N., 2019. Deformation based morphometry study of longitudinal MRI changes in behavioral variant frontotemporal dementia. *NeuroImage Clin* 24, 102079.
- Manera, A.L., Dadar, M., Fonov, V., Collins, D.L., 2020. CerebRA, registration and manual label correction of Mindboggle-101 atlas for MNI-ICBM152 template. *Sci. Data* 7, 1–9.
- Manera, A.L., Dadar, M., Van Swieten, J.C., Borroni, B., Sanchez-Valle, R., Moreno, F., Laforce, R., Graff, C., Synofzik, M., Galimberti, D., 2021. MRI data-driven algorithm for the diagnosis of behavioural variant frontotemporal dementia. *J. Neurol. Neurosurg. Psychiatry* 92, 608–616.
- McAlease, K.E., Alafuzoff, I., Charidimou, A., De Reuck, J., Grinberg, L.T., Hainsworth, A.H., Hortobagyi, T., Ince, P., Jellinger, K., Gao, J., 2016. Post-mortem assessment in vascular dementia: advances and aspirations. *BMC Med* 14, 129.
- Misquitta, K., Dadar, M., Louis Collins, D., Tartaglia, M.C., 2020. White matter hyperintensities and neuropsychiatric symptoms in mild cognitive impairment and Alzheimer's disease. *NeuroImage Clin* 28, 102367. doi:10.1016/j.nicl.2020.102367.
- Piccini, P., Pavese, N., Canapicchi, R., Paoli, C., Dotto, P.D., Puglioli, M., Rossi, G., Bonuccelli, U., 1995. White matter hyperintensities in Parkinson's Disease: clinical correlations. *Arch. Neurol* 52, 191–194. doi:10.1001/archneur.1995.00540260097023.
- Prins, N.D., Scheltens, P., 2015. White matter hyperintensities, cognitive impairment and dementia: an update. *Nat. Rev. Neurol* 11, 157–165.
- Rizvi, B., Lao, P.J., Colón, J., Hale, C., Igwe, K.C., Narkhede, A., Budge, M., Manly, J.J., Schupf, N., Brickman, A.M., 2020. Tract-defined regional white matter hyperintensities and memory. *NeuroImage Clin* 25, 102143. doi:10.1016/j.nicl.2019.102143.
- Sanford, R., Strain, J., Dadar, M., Maranzano, J., Bonnet, A., Mayo, N.E., Scott, S.C., Fellows, L.K., Ances, B.M., Collins, D.L., 2019. HIV infection and cerebral small vessel disease are independently associated with brain atrophy and cognitive impairment. *AIDS Lond. Engl* 33, 1197–1205. doi:10.1097/QAD.0000000000002193.
- Sluimer, J.D., van der Flier, W.M., Karas, G.B., van Schijndel, R., Barnes, J., Boyes, R.G., Cover, K.S., Olabarriaga, S.D., Fox, N.C., Scheltens, P., Vrenken, H., Barkhof, F., 2009. Accelerating regional atrophy rates in the progression from normal aging to Alzheimer's disease. *Eur. Radiol* 19, 2826. doi:10.1007/s00330-009-1512-5.
- Spulber, G., Niskanen, E., MacDonald, S., Kivipelto, M., Ferreira Padilla, D., Julkunen, V., Hallikainen, M., Vanninen, R., Wahlund, L.-O., Soininen, H., 2012. Evolution of global and local grey matter atrophy on serial MRI scans during the progression from MCI to AD. *Curr. Alzheimer Res* 9, 516–524.
- Sudre, C.H., Bocchetta, M., Heller, C., Convery, R., Neason, M., Moore, K.M., Cash, D.M., Thomas, D.L., Woollacott, I.O.C., Foiani, M., Heslegrave, A., Shafei, R., Greaves, C., van Swieten, J., Moreno, F., Sanchez-Valle, R., Borroni, B., Laforce, R., Masellis, M., Tartaglia, M.C., Graff, C., Galimberti, D., Rowe, J.B., Finger, E., Synofzik, M., Vandenberghe, R., de Mendonça, A., Tagliavini, F., Santana, I., Ducharme, S., Butler, C., Gerhard, A., Levin, J., Danek, A., Frisoni, G.B., Sorbi, S., Otto, M., Zetterberg, H., Ourselin, S., Cardoso, M.J., Rohrer, J.D., Rossor, M.N., Warren, J.D., Fox, N.C., Guerreiro, R., Bras, J., Thomas, D.L., Nicholas, J., Mead, S., Jiskoot, L., Meeter, L., Panman, J., Pappa, J., van Minkelen, R., Pijnenburg, Y., Barandiaran, M., Indakoetxea, B., Gabilondo, A., Tainta, M., Arriba, M., de Gorostidi, A., Zulaica, M., Villanua, J., Diaz, Z., Borrego-Ecija, S., Olives, J., Lladó, A., Balasa, M., Antonell, A., Bargallo, N., Premi, E., Cosseddu, M., Gazzina, S., Padovani, A., Gasparotti, R., Archetti, S., Black, S., Mitchell, S., Rogeava, E., Freedman, M., Keren, R., Tang-Wai, D., Öijerstedt, L., Andersson, C., Jelic, V., Thonberg, H., Arighi, A., Fenoglio, C., Scarpini, E., Fumagalli, G., Cope, T., Timberlake, C., Rittman, T., Shoesmith, C., Bartha, R., Rademakers, R., Wilke, C., Karnarh, H.-O., Bender, B., Bruffaerts, R., Vandamme, P., Vandenbulcke, M., Ferreira, C.B., Miltenberger, G., Maruta, C., Verdelho, A., Afonso, S., Taipa, R., Caroppo, P., Di Fede, G., Giaccone, G., Prioni, S., Redaelli, V., Rossi, G., Tiraboschi, P., Duro, D., Almeida, M.R., Castelo-Branco, M., Leitão, M.J., Tabuas-Pereira, M., Santiago, B., Gauthier, S., Rosa-Neto, P., Veldsman, M., Flanagan, T., Prix, C., Hoegen, T., Wlasich, E., Loosli, S., Schonecker, S., Semler, E., Anderl-Straub, S., Benussi, L., Binetti, G., Ghidoni, R., Pievani, M., Lombardi, G., Nacmias, B., Ferrari, C., Bessi, V., 2019. White matter hyperintensities in progranulin-associated frontotemporal dementia: a longitudinal GENFI study. *NeuroImage Clin* 24, 102077. doi:10.1016/j.nicl.2019.102077.
- Tosto, G., Zimmerman, M.E., Carmichael, O.T., Brickman, A.M., 2014. Predicting aggressive decline in mild cognitive impairment: the importance of white matter hyperintensities. *JAMA Neurol* 71, 872–877.
- Tuladhar, A.M., Reid, A.T., Shumskaya, E., de Laat, K.F., van Norden, A.G.W., van Dijk, E.J., Norris, D.G., de Leeuw, F.-E., 2015. Relationship between white matter hyperintensities, cortical thickness, and cognition. *Stroke* 46, 425–432. doi:10.1161/STROKEAHA.114.007146.
- Varma, A.R., Laitt, R., Lloyd, J.J., Carson, K.J., Snowden, J.S., Neary, D., Jackson, A., 2002. Diagnostic value of high signal abnormalities on T2 weighted MRI in the differentiation of Alzheimer's, frontotemporal and vascular dementias. *Acta Neurol. Scand* 105, 355–364. doi:10.1034/j.1600-0404.2002.01147.x.
- Vipin, A., Foo, H.J.L., Lim, J.K.W., Chander, R.J., Yong, T.T., Ng, A.S.L., Hameed, S., Ting, S.K.S., Zhou, J., Kandiah, N., 2018. Regional white matter hyperintensity influences grey matter atrophy in mild cognitive impairment. *J. Alzheimers Dis* 66, 533–549. doi:10.3233/JAD-180280.
- Wen, W., Sachdev, P.S., Chen, X., Anstey, K., 2006. Gray matter reduction is correlated with white matter hyperintensity volume: a voxel-based morphometric study in a large epidemiological sample. *NeuroImage* 29, 1031–1039.
- Whitwell, J.L., Boeve, B.F., Weigand, S.D., Senjem, M.L., Gunter, J.L., Baker, M.C., DeJesus-Hernandez, M., Knopman, D.S., Wszolek, Z.K., Petersen, R.C., Rademakers, R., Jack, C.R., Josephs, K.A., 2015. Brain atrophy over time in genetic and sporadic frontotemporal dementia: a study of 198 serial magnetic resonance images. *Eur. J. Neurol* 22, 745–752. doi:10.1111/ene.12675.
- Woollacott, I.O.C., Bocchetta, M., Sudre, C.H., Ridha, B.H., Strand, C., Courtney, R., Ourselin, S., Cardoso, M.J., Warren, J.D., Rossor, M.N., Revesz, T., Fox, N.C., Holton, J.L., Lashley, T., Rohrer, J.D., 2018. Pathological correlates of white matter hyperintensities in a case of progranulin mutation associated frontotemporal dementia. *Neurocase* 24, 166–174. doi:10.1080/13554794.2018.1506039.
- Xie, C., Bai, F., Yu, H., Shi, Y., Yuan, Y., Chen, G., Li, W., Chen, G., Zhang, Z., Li, S.J., 2012. Abnormal insula functional network is associated with episodic memory decline in amnesic mild cognitive impairment. *NeuroImage* 63, 320–327. doi:10.1016/j.neuroimage.2012.06.062.
- Yeh, F.-C., Panesar, S., Fernandes, D., Meola, A., Yoshino, M., Fernandez-Miranda, J.C., Vettel, J.M., Verstynen, T., 2018. Population-averaged atlas of the macroscale human structural connectome and its network topology. *NeuroImage* 178, 57–68. doi:10.1016/j.neuroimage.2018.05.027.
- Yoshita, M., Fletcher, E., Harvey, D., Ortega, M., Martinez, O., Mungas, D.M., Reed, B.R., DeCarli, C.S., 2006. Extent and distribution of white matter hyperintensities in normal aging, MCI, and AD. *Neurology* 67, 2192–2198.
- Zeighami, Y., Fereshtehnejad, S.-M., Dadar, M., Collins, D.L., Postuma, R.B., Dagher, A., 2019. Assessment of a prognostic MRI biomarker in early de novo Parkinson's disease. *NeuroImage Clin* 24, 101986.
- Zeighami, Y., Ulla, M., Iturria-Molina, Y., Dadar, M., Zhang, Y., Larcher, K.M.-H., Fonov, V., Evans, A.C., Collins, D.L., Dagher, A., 2015. Network structure of brain atrophy in de novo Parkinson's disease. *elife* 4, e08440.